

## Drug substance manufacture process control: application of flow injection analysis and HPLC for monitoring an enantiospecific synthesis

K. Chong, T. Loughlin, C. Moeder, H.J. Perpall, R. Thompson, N. Grinberg\*,  
G.B. Smith, M. Bhupathy, G. Bicker

*Merck Research Laboratories, P.O. Box 2000, R80Y-115 Rahway, NJ 07065-0900, USA*

Received for review 5 October 1995; revised manuscript received 1 February 1996

### Abstract

Effective process control can only be achieved through an understanding of the operating issues of the reaction. The development and use of effective and rugged analytical methods is necessary to monitor these parameters. The intent of this paper is to present some key analytical issues encountered in the synthesis of MK-0679, an LTD<sub>4</sub> antagonist. In a key step of the compound's synthesis, a prochiral diester intermediate undergoes an enantioselective enzymatic hydrolysis (in the presence of Triton X-100) leading to the (*S*)-ester acid. Subsequent processing transforms the ester acid into the final product. The residual amount of the detergent in the final product, the rapid determination of the enzymatic activity and the optical purity of the final product emerged as key issues in the control of the reaction. As a solution, two techniques were utilized and are presented: flow injection analysis and HPLC.

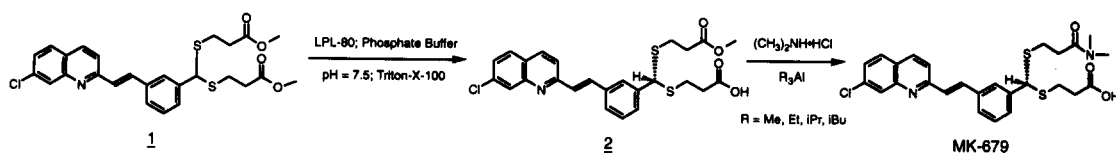
*Keywords:* Diastereomers; Enantiomeric separation; Enzyme activity; Flow injection

### 1. Introduction

The stereochemistry of a drug can play an important role on its biological activity, toxicology and metabolism. Tremendous differences in these properties have been observed for the enantiomers of chiral drugs [1–3]. Based upon recent projections [4–6] and general regulatory guidelines [5–11], chiral drugs marketed as racemates will be considered as combinations of individual entities

or enantiomers. As a result, many pharmaceutical companies are evaluating the biological activity, toxicity and metabolism of each enantiomer in the early stages of racemic drug development [12]. In many cases, this approach to development leads to the production of enantiomerically pure drugs through the use of asymmetric synthesis [13], catalytic kinetic resolution [14], resolution of racemates through stereoselective crystallization [15], chiral chromatography [16] and biocatalytic processes [1,17,18]. Biocatalytic processes feature the use of enzymes as enantiomeric discriminators of racemic substrates [19–26].

\* Corresponding author. Tel: (908) 594-5055; fax: (908) 594-5468.



Scheme 1. Synthetic pathway for MK-0679.

MK0679, a leukotriene  $D_4$  antagonist [27], is enantioselectively prepared utilizing lipases derived from *Pseudomonas* species [28–31]. The drug's chiral center is generated through the enzymatic hydrolysis of the prochiral diester to the (*S*)-ester acid, the penultimate of MK0679. Scheme 1 describes the synthetic pathway for MK-0679 starting from the diester **1**. In the presence of the lipase LPL80 under aqueous buffer conditions at pH 7.5, the diester **1** undergoes a selective enzymatic hydrolysis to the ester **2**. To insure that the reaction is performed in a homogeneous medium and to enhance the solubility of **1**, Triton X-100 (T-X) was added as a surfactant at a concentration above the critical micelle concentration. After **2** has been isolated as a solid, it undergoes an aqueous wash to remove T-X. Monitoring the residual amounts of T-X in both solid and liquid samples is necessary in order to establish the number of washes required for the removal of the detergent. In addition, the determination of the enzyme activity is also necessary in order to ascertain the number of cycles that the enzyme can be reused during the hydrolysis step. The ester acid **2** is reacted with dimethyl amine to form the final product MK0679. Theoretically, during this step of the reaction, some racemization may occur, and consequently the determination of the optical purity of the final product is required. From an analytical point of view, three issues are to be solved: the determination of the enzyme activity, the determination of T-X and the determination of the enantiomeric purity of the final product.

The three analytical methods reported here are used in the manufacturing process control of the MK0679 drug substance. The first method is a flow injection analysis (FI) method, which evaluates the lipase activity. Another FI method for the determination of Triton X-100, a surfactant in the reaction medium, utilizes an on-line solid-phase

cation-exchange extractor [32]. The third method involves the determination of the MK0679 enantiomeric purity through the formation of naphthylethylamine diastereomers and their separation on a chiral (*R*)-urea bonded phase.

## 2. Materials and methods

### 2.1. Reagents

MOPS and HEPES were purchased from Sigma (St. Louis, MO). Hexane, triethylamine, acetonitrile, isobutyl alcohol and 2-propanol (HPLC grade), Triton X-100 and phosphoric acid were purchased from Fisher Scientific (Springfield, NJ). MK0679 and the intermediates **1** and **2** were obtained from the Process Research Department (Merck Research Laboratories, Rahway, NJ). The lipase enzyme from *Pseudomonas cepacia* was purchased from Amano Enzyme Co. (Japan). (*S*)-Naphthylethylamine and ethyl chloroformate were purchased from Aldrich (Milwaukee, WI).

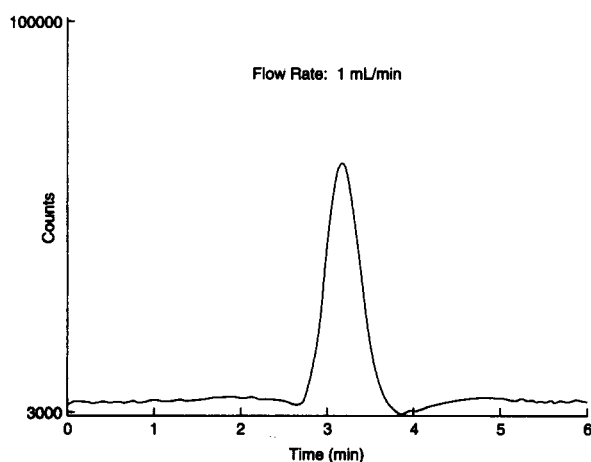


Fig. 1. Detector response after injecting  $10 \mu\text{l}$  of  $0.5 \text{ mg ml}^{-1}$  solution of lipase into the FI system.

Table 1  
Influence of flow rate on the peak area and RT

Flow rate (ml min <sup>-1</sup> )	Peak area (counts)	RT (min)
0.80	5 740 405	4.81
0.70	6 314 763	5.48
0.50	8 266 183	7.62
0.30	23 698 369	13.17
0.20	36 607 899	19.56
0.10	66 894 177	38.78
0.05	161 764 822	76.51

## 2.2. Apparatus

The FI system used for the determination of the enzyme activity consisted of a Beckman model 126 HPLC pump, a Beckman model 507 autosampler (Fullertown, CA) equipped with a Rheodyne model 7126 injection valve, a knitted PTFE reactor (0.5 mm × 15 m) (Aura Industries, Staten Island, NY) and a Waters conductivity detector (Milford, MA).

The FI system used for the determination of Triton X-100 consisted of a Varian Vista 5500 liquid chromatograph (Walnut Creek, CA, USA) equipped with a Varian UV-200 variable-wavelength detector and a Varian model 8085 autosampler with a 20 μl loop. The solid-phase extractor consisted of a Whatman Partisil 10 SCX strong cation-exchange high-performance liquid chromatographic column (25 × 0.46 cm i.d.) (Maidstone, Kent, UK).

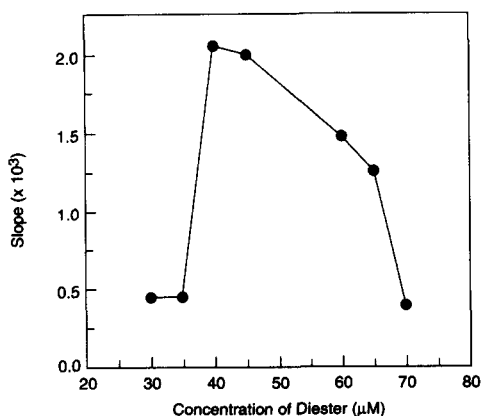


Fig. 2. Influence of the concentration of **1** on the slopes.

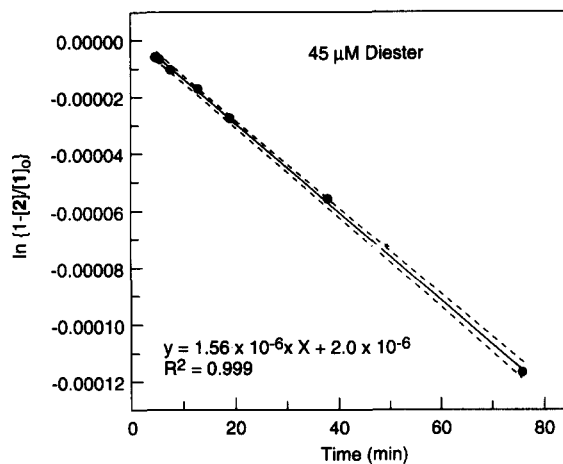


Fig. 3. Kinetics of the hydrolysis of **1** when its concentration in the carrier was 45 μM.

The enantiomeric separation of the MK-0679 final product was performed on a Spectra-Physics system (San Jose, CA, USA) equipped with SP8800 pumps and an SP8775 autosampler equipped with a Rheodyne valve with a 10 μl loop. For the detection of the two enantiomers, a Spectroflow 757 absorbance detector (Applied Biosystem, Foster City, CA) was used.

All the data were collected and analyzed with a PE Nelson Access Chrom chromatography data acquisition system (Cupertino, CA, USA).

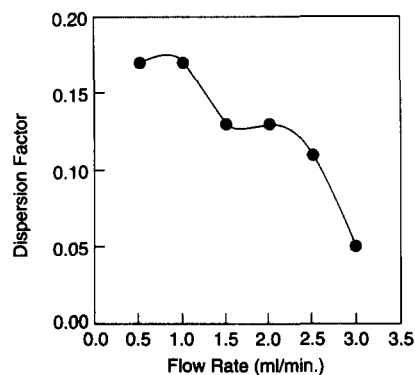


Fig. 4. Influence of flow rate on the dispersion factor of T-X. Carrier composition: 65% 5 mM KH<sub>2</sub>PO<sub>4</sub> (pH 2), 35% isobutyl alcohol–acetonitrile (50:50, v/v). Detection: UV at 276 nm.

Table 2  
Influence of organic modifier on the retention of the intermediates<sup>a</sup>

Organic modifier (%)	Retention time (min)
30	4.55
32	3.98
35	3.32
38	3.26
40	3.23
42	3.11

<sup>a</sup> The intermediates elute as a single peak.

#### 2.4. FI analysis for the enzyme activity assay

The carrier used for the determination of the lipase activity consisted of a buffer containing 5 mM MOPS, 5 mM HEPES, 15% Triton X-100 and various concentrations of **1**. The pH of the buffer was adjusted to 7.5 with sodium hydroxide. The enzyme solution was prepared by dissolving the lipase in carrier solution without **1** to obtain a concentration of 0.5 mg ml<sup>-1</sup>; 10 μl of the lipase solution were introduced into the FI system. Lipase activity was then determined from the magnitude of the peak caused by the formation of **2**.

#### 2.5. FI analysis for the determination of Triton X-100

The carrier used for the determination of Triton X-100 consisted of two solutions: (A) 5 mM KH<sub>2</sub>PO<sub>4</sub>, the pH of which was adjusted to 2.0 with orthophosphoric acid, and (B) isobutyl alcohol–acetonitrile (50:50, v/v). Solutions A and B were pump mixed in the ratio 65:35 (v/v).

Table 3  
Influence of ionic strength of the carrier on the retention of the intermediates<sup>a</sup>

Ionic strength (mol l <sup>-1</sup> )	Retention time (min)
0.005	3.35
0.010	2.35
0.015	1.89

<sup>a</sup> The intermediates elute as a single peak.

The monitoring of T-X was performed at 276 nm. Samples of isolated intermediate **2** were prepared by dissolving approximately 200 mg of solid sample in 10 ml of the carrier. A heat gun and a sonicating bath were used to aid in the dissolution. When the temperature returned to ambient, the samples were passed through a Genex 0.25 μm PTFE filter (Gaithersburg, MD, USA) and introduced into the FI system. If the samples were liquid, 1–5 ml were introduced into 10 ml calibrated flasks and an aliquot (3.5 ml) of solution B was added to the contents of each flask. The mixture was diluted to the mark with solution A and passed through a Genex 0.25 μm PTFE filter prior to introduction into the FI system. The matrix is retained by the solid extractor, leading to its separation from T-X.

#### 2.6. Determination of enantiomeric purity of MK0679

The chromatographic chiral separation of MK0679 and its enantiomer was performed on a Supelco LC-(R)-Urea column (Supelco, Bellefonte, PA, USA) (25 × 0.46 cm i.d.) packed with a 5 μm particle size material. The mobile phase used for the separation of the enantiomers consisted of two solutions: (A) 0.3% triethylamine in hexane and (B) 2-propanol–acetonitrile (50:50, v/v). Solutions A and B were pump mixed in the ratio 95:5 (v/v). The two enantiomers were derived with (*S*)-naphthylamine according to the following procedure: 10 mg of each enantiomer were introduced into a 10 ml vial and dissolved in 2 ml of tetrahydrofuran using vortex mixing to aid in the dissolution. A 100 μl of 0.2 M triethylamine dissolved in acetonitrile followed by a 100 μl aliquot of 0.2 M ethyl chloroformate dissolved in acetonitrile were added to the vial. The reaction mixture was vortex mixed and allowed to react for 10 mins. The solvent was evaporated under nitrogen and reconstituted in 3 ml of ethanol. An aliquot of 10 μl of this solution was introduced into the HPLC system. The detection of the two diastereomers was performed by UV spectrophotometry at 278 nm.

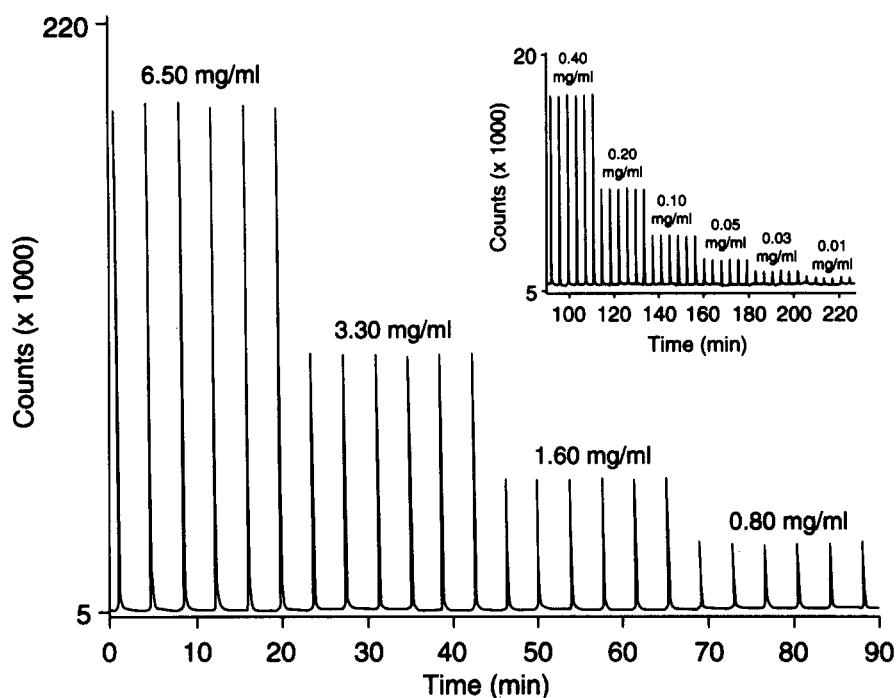


Fig. 5. Repeatability of FI for T-X. FI conditions as in Fig. 4. Numbers above peaks are concentrations of T-X.

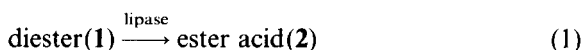
### 3. Results and discussion

#### 3.1. Determination of enzyme activity

From an analytical process point of view, the determination of the lipase activity must be a rapid, rugged and reproducible assay. To determine the enzyme activity, a flow injection (FI) approach was selected. For this analysis, **1** was dissolved in the carrier and continuously pumped through the system. The pH of the carrier was adjusted to 7.5. At this pH, the conductivity of the buffer was insignificant. The enzyme is introduced into the system, as a discrete injection plug, the hydrolysis process begins and **2** is obtained. At the working pH, the carboxyl group is totally deprotonated and it can be detected by the conductivity detector. The effect of an injection of 10  $\mu\text{l}$  of enzyme solution into the system is depicted in Fig. 1. Variation of the flow rate produces a variation of the reaction time between enzyme and **1**. Table 1 shows that the peak area of **2** decreases

with increasing flow rate, owing to a decrease in the residence time (RT) of lipase in the system.

A plot of RT vs. the area counts of the peak proved to be linear with  $r^2 = 0.999$ . The concentration of **1** in the carrier was varied from 30 to 70  $\mu\text{M}$ . For all of the concentrations, plots of RT vs. area counts proved to be linear with  $r^2 > 0.99$ . The slopes of the plots, at various concentrations of **1** in the carrier, are related to the rates of the reaction. Fig. 2 shows the relationship of the concentrations of **1** to the slopes of the lines. A maximum was obtained between 40 and 45  $\mu\text{M}$  of **1** in the carrier. The decrease in the slopes observed at higher concentrations of **1** is consistent with an enzymatic inhibition by substrate [32]. The rate constant was determined where the reaction rate was maximum. Under these circumstances, if it is considered that the reaction



proceeds irreversibly to completion, then the rate law is [33]

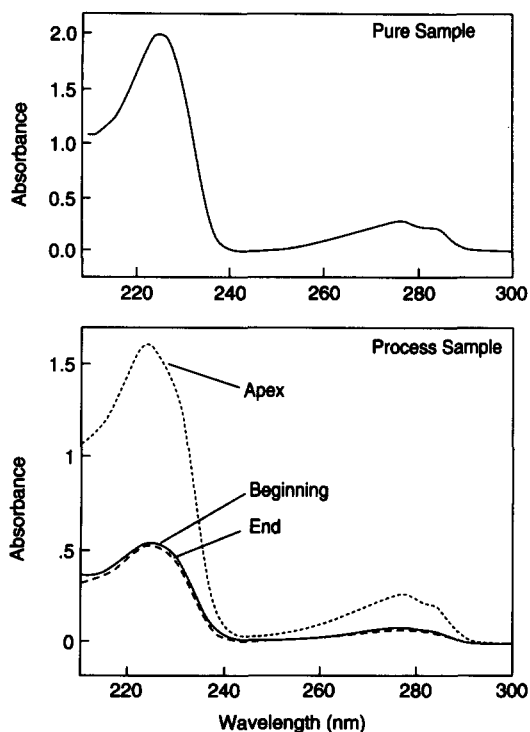


Fig. 6. Top: UV spectrum of pure T-X dissolved in the carrier described in Fig. 4. Bottom: UV spectra of T-X peak from a process sample obtained through FI using a Waters photodiode-array detector. For FI conditions, see Fig. 4.

$$-d[1]/dt = k[1] \quad (2)$$

Eq. (2) can be solved by integration between the time limits  $t_0$ , taken as zero, and time  $t$  and between the concentrations  $[1]_0$  and  $[1]$ . The inte-

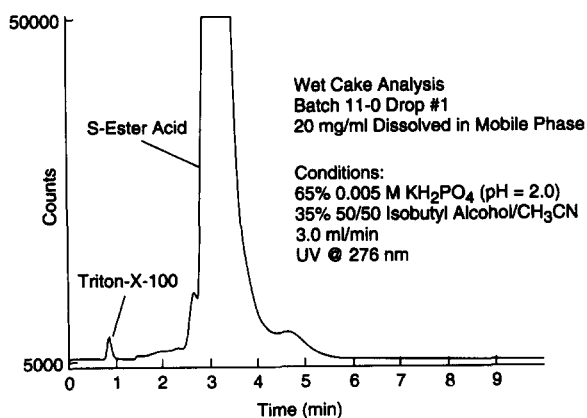


Fig. 7. FI trace of a solid sample. For FI conditions, see Fig. 4.

Table 4

Comparison of the results obtained from the calibration graph and standard addition

Sample	Concentration of T-X determined ( $\text{mg ml}^{-1}$ )	
	Calibration graph	Standard addition
Solid samples		
1	0.09	0.10
2	0.07	0.07
3	0.15	0.14
4	0.10	0.10
Liquid samples		
Supernatant	16.82	16.53
Filtrate	16.52	16.60
Aqueous wash	9.12	9.07

grated rate expression has the form

$$[1] = [1]_0 \exp(-kt) \quad (3)$$

An alternative to Eq. (3) can be written when the concentration of 2 is used as a variable instead of  $[1]$ . Thus, considering that  $[1] + [2] = [1]_0$ , Eq. (3) becomes

$$[2] = [1]_0 [1 - \exp(-kt)] \quad (4)$$

or

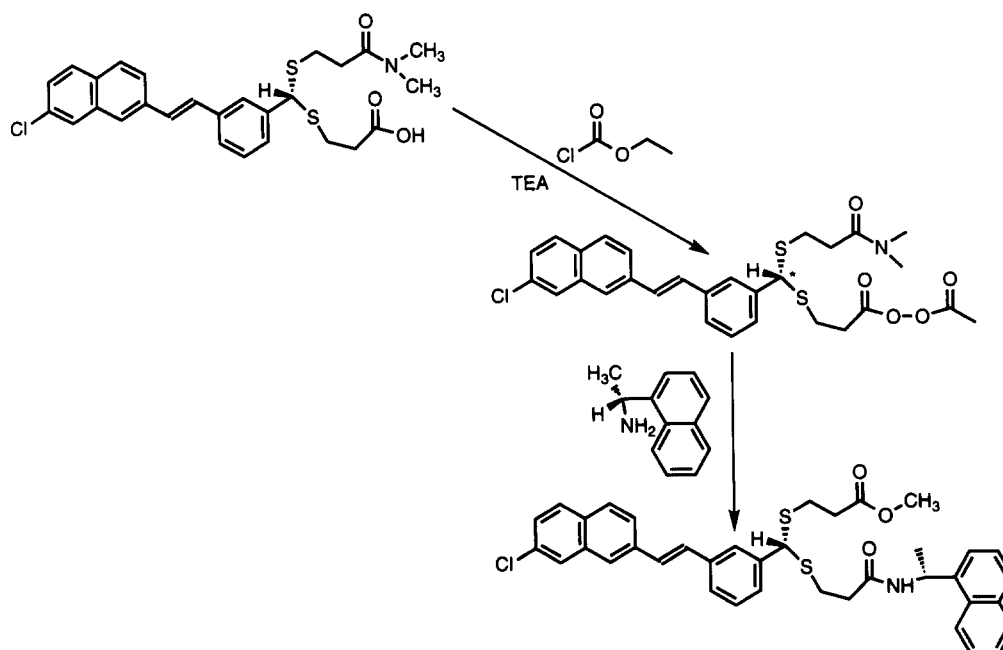
$$\ln\{1 - ([2]/[1]_0)\} = -kt \quad (5)$$

Eq. (5) predicts that a plot of  $\ln\{1 - ([2]/[1]_0)\}$  vs. time should be a straight line with a slope  $k$ , which is the rate constant of the reaction.

The plot of  $\ln\{1 - ([2]/[1]_0)\}$  vs. time is linear ( $r^2 = 0.999$ ) and is presented in Fig. 3. Since every point investigated has the same rate constant, a 5 min assay (minimum reaction time investigated) can be achieved. The rate constant obtained from the FI experiments was comparable with that obtained using batch experiments [30].

Lipase activity was calculated as follows. A sample of lipase was introduced into the system at a flow rate of  $1 \text{ ml min}^{-1}$ . The generated peak area was correlated with ester acid concentration obtained from a calibration curve. Assuming a first-order reaction and a one to one stoichiometry, the lipase activity was calculated as [34]

$$\text{specific activity} = \text{units/g lipase} \quad (6)$$



Scheme 2. Derivatization pathway for MK-0679. For conditions, see Materials and methods section.

where one unit of enzyme activity is defined as the enzyme quantity which produces 1  $\mu\text{mol}$  of product in 1 min. Using this assay, a lot of lipase was analyzed and the activity was determined to be 800 000 units  $\text{g}^{-1}$ , which was in agreement with the manufacturer's specification of 813 000 units  $\text{g}^{-1}$ . The relative standard deviation of the analysis was 0.5%.

### 3.2. Determination of Triton X-100

Triton X-100 (T-X) is a non-ionic surfactant and appears as a mixture of oligomers. Determination of this surfactant by chromatographic methods requires the summation of the area under a number of peaks. Such an approach is cumbersome owing to the complexity of the mixture. FI with an on-line strong cation-exchange solid-phase extractor was found to be a useful technique for the quantitation of the surfactant. The extractor retains the MK-0679 components while allowing the T-X through unretained for quantitation. In this sense, analysis of this type falls into the FI category.

Reviewing the reaction in Scheme 1, a common functionality of all the components in the reaction is the quinoline ring. The  $\text{pK}_a$  of the quinoline nitrogen was determined by non-aqueous titration to be 5.06 [35]. Using a carrier of pH 2.0, all the quinoline derivatives will be retained on the extractor. The T-X will be uncharged and pass through the extractor unretained.

In defining the optimum conditions for FI, the flow rate of the carrier stream is important. An increase in the flow rate will lead to a short residence time of the analyte in the FI system. Since T-X is quantified in the dead volume of the extractor, an increase in the flow rate will also minimize the axial diffusion of the compound in the carrier. A small axial diffusion will lead to a sharper peak and consequently a better detection limit. A low dispersion factor is considered as a measure of the T-X peak sharpness [36] and, under our experimental conditions, this phenomenon can be easily seen (Fig. 4). As the flow rate increases, the dispersion factor of the T-X peak decreases, resulting in a better detection limit.

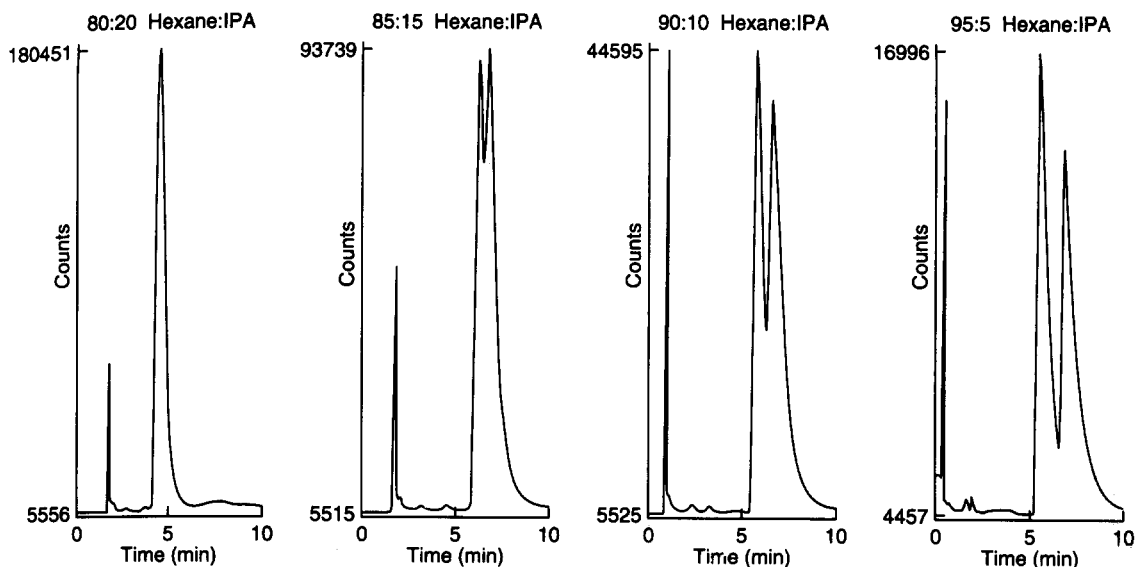


Fig. 8. Influence of IPA concentration on the separation between the two enantiomers of MK-0679.

The solid-phase extractor used in our experiments consisted of a strong cation exchanger. Special care was taken to establish the conditions under which the intermediates were retained on the extractor. One factor that influences the interaction between MK-0679 intermediates and the solid-phase extractor is the amount of organic modifier [isobutyl alcohol–acetonitrile (50:50, v/v)] in the carrier. As the amount of modifier in the carrier stream increases, the intermediates and the solid support are solvated and their interaction with the extractor is diminished. The carrier stream composition was adjusted such that all the intermediates would elute as a single peak that is well resolved from the T-X. The data in Table 2 show that, as the composition of the organic modifier increases, the retention of the intermediates decreases. In order to keep the analysis time short, a level of 35% organic modifier was chosen. This organic modifier concentration provides for fast analysis without compromising the separation between the T-X peak and the intermediates peak.

Increasing the ionic strength of the carrier led to a shielding of the electrostatic interaction between the intermediates and the solid support (Table 3). At high ionic strengths a decreased retention of the intermediates could lead to potential contamination of the T-X peak because of peak co-elution.

A  $\text{pH}_{\text{app}}$  of 2.00 and 5 mM  $\text{K}_2\text{PO}_4$  in the carrier were selected to achieve a reasonable retention of the intermediates on the extractor.

The spectra of T-X indicates that it has absorption maxima at 255 and 276 nm. Because of the interference of the carrier in low-UV region, a wavelength of 276 nm was chosen for the detection of the analyte. A series of T-X concentrations ranging from 0.01 to 6.50  $\text{mg ml}^{-1}$  were prepared under the conditions described under Experimental (Fig. 5). A least-squares treatment of the data indicated a linear correlation ( $y = 221\,399.7x + 324.7$ ,  $r^2 = 0.9999$ ). Since the data covered a concentration range over two orders of magnitude, the linearity was checked in the lower range of the graph (0.01–0.20  $\text{mg ml}^{-1}$ ) and  $r^2 = 0.9999$  was also obtained. A detection limit of 0.005  $\text{mg ml}^{-1}$  was obtained at a signal-to-noise ratio of 3:1.

With the FI system optimized, the next step was to evaluate the sample preparation. Since T-X is a surfactant with a tendency to interact with many different surfaces, it was necessary to establish that the T-X was not retained on the PTFE membrane filters. A range of T-X solutions with concentrations from 0.06 to 5  $\text{mg ml}^{-1}$  were prepared. The solutions were passed through the PTFE filter and analyzed before and after filtration. A straight line was obtained with a slope of



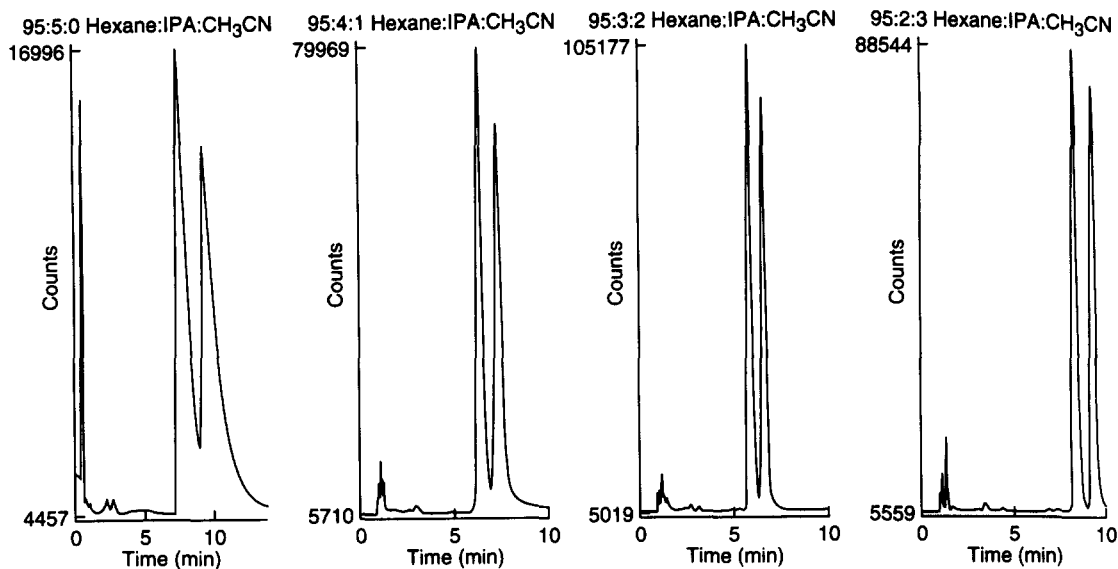


Fig. 9. Influence of the addition of acetonitrile to the mobile phase on the separation of the two enantiomers of MK-0679.

unity and an intercept of zero, indicating that T-X was not retained on the filter.

With the solid samples (isolated intermediates), where the amount of T-X was expected to be below the detection limit, a large sample size (ca. 20 mg mL<sup>-1</sup>) was needed to bring the T-X concentration into the range of the calibration graph. To prove that there was no co-elution of the intermediates with the T-X peak under these overloading condi-

tions, it was necessary to check the T-X peak purity. By using a Waters Model 991 photodiode-array detector, spectra of the T-X peak were taken at the front, apex and end of the peak. The spectra obtained indicated peak homogeneity. These spectra were compared with the spectrum of a pure T-X sample taken on an AVIV Model 118DS spectrophotometer. The results are presented in Fig. 6. The three sets of spectra are identical, indicating that no co-elution of the MK-0679 intermediates occurred. A typical trace of a solid sample is presented in Fig. 7.

The validation for the determination of T-X was performed on actual process samples. The samples were prepared as described under Experimental. The amount of T-X was determined in two ways, first by using a calibration curve and second by using a standard addition method. With the standard addition method, an amount of T-X equivalent to 25% of the amount determined by the calibration curve was added to each sample. Each sample was then injected twice, with and without T-X added. The concentration was calculated according to

$$S_y = (A' - A)/M_y$$

$$Y = A/S_y$$

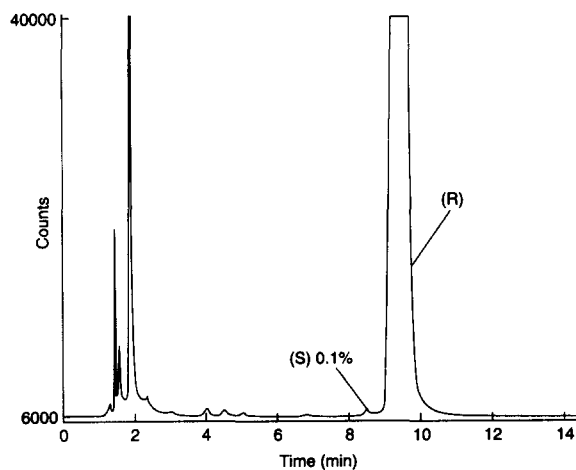


Fig. 10. Separation of MK-0679 from its enantiomer at a level of 99.9:0.1. For experimental conditions, see Materials and methods section.

where  $S_y$  is the calibration factor,  $A$  is the peak area of the sample without the standard addition,  $A'$  is the peak area of the sample with the standard addition,  $M_y$  is the mass of T-X added and  $Y$  is the mass of T-X is the unknown sample.

The result of the comparison of the two methods are presented in Table 4 and show good agreement.

### 3.3. Determination of the enantiomeric purity of MK-0679

The determination of the enantiomeric purity of the compound using several direct separation methods was attempted. The results of the separations were unsuccessful. The separation was futile owing to the position of the functional groups from the chiral center able to undergo interaction with a chiral phase. Therefore, an indirect method was pursued.

The approach consisted of the formation of an active ester of MK-0679 by reacting MK-0679 with ethyl chloroformate. The ester formed was reacted with a chiral reagent, naphthylethylamine, to form a diastereomer (Scheme 2). If the enantiomeric purity of the amine is high, then the separation of the two diastereomers of MK-0679 will correspond to the separation of the two enantiomers of MK-0679. The attempts to separate the resulted diastereomers under achiral reversed-phase HPLC [28] conditions led to very broad peaks, allowing the determination of only 2% of the minor diastereomer. Achiral normal-phase conditions for the separation of the two diastereomers also proved to be unsuccessful.

A new approach using the derivatized compound was attempted by trying the separation on a chiral column. Examination of the derivatized compound shows that the compound contains an amide bond at the derivatized functional group. To achieve the separation, a chiral phase should be chosen to complement the amide group by interaction through hydrogen bonding. Therefore, a urea column was selected which can undergo hydrogen bonding at the carbodiimide functionality as the leading interaction. A mobile phase consisting of a hexane–2-propanol (IPA)

was selected. The effect of variation of the percentage of IPA in hexane is shown in Fig. 8. Hexane–IPA (95:5, v/v) was selected for further optimization because at this composition the best resolution was produced. However, the peak shape was broad and the resolution was not baseline. To improve the peak shape, acetonitrile was added to the mobile phase. The increase in the acetonitrile concentration was performed at the expense of IPA concentration, such that the final concentration of the polar components was kept constant at 5%. The results are presented in Fig. 9. The best separation of the two enantiomers was achieved with a mobile phase consisting of hexane–IPA–acetonitrile (95:2:3, v/v/v). Under these conditions, the separation was baseline, and allowed the determination of 0.1% of the minor enantiomer (Fig. 10). No interferences or bias was observed in the chromatography due to the derivatization procedure. Spiking experiments showed complete recovery.

## 4. Conclusions

The critical analytical issues for in-process testing of MK-0679 were the determination of the enzyme activity, determination of T-X and determination of the enantiomeric purity of MK-0679 final product. The use of flow injection for the determination of enzyme activity was demonstrated and the experimental results were comparable to those of the batch experiments. The method used for the determination of T-X provided rapid and accurate results. Standard addition and calibration curve methods correlated well for the determination of T-X. Lastly, the determination of the enantiomeric purity of MK-0679 final product was achieved using a mixed approach, derivatization of the compound with a chiral reagent and the separation of the two diastereomers on a chiral column. The use of this method allowed for the determination of 0.1% by area of the minor enantiomer as compared with the major enantiomer. With the use of the methods described, a good overall understanding of the issues of the synthesis was established.

**References**

- [1] B. Testa and M. Mayer, *Prog. Drug Res.*, 32 (1988) 249–303.
- [2] A. Beckett, *Biochem. Soc. Trans.*, 19 (1991) 443–446.
- [3] E.J. Ariens, *Med. Res. Rev.* 6 (1986) 451–466.
- [4] E.J. Ariens, E.W. Wuis and E.J. Veringa, *Biochem. Pharmacol.*, 37 (1988) 9–18.
- [5] M.N. Cayen, *Chirality*, 3 (1991) 94–98.
- [6] J.H.G.M. Mustaers and H.J. Kooreman, *Rec. Trav. Chim. Pays-Bas*, 110 (1991) 185–188.
- [7] W.H. Decamp, *Chirality*, 1 (1989) 2–6.
- [8] J. Weissinger, *Drug Info. J.*, 23 (1989) 663–667.
- [9] M. Goss, *Annu. Rep. Med. Chem.*, 25 (1989) 323–331.
- [10] H. Shindo and J. Caldwell, *Chirality*, 3 (1991) 91–93.
- [11] A.C. Cartwright, *Biochem. Soc. Trans.*, 19 (1991) 465–467.
- [12] D.B. Campbell and K. Wilson, *Biochem Soc. Trans.*, 19 (1991) 472–475.
- [13] J.M. Brown and S.G. Davis, *Nature (London)*, 342 (1989) 631–636.
- [14] H.B. Kagan and J.C. Fiaud, *Top. Stereochem.*, 18 (1988) 249–330.
- [15] R. Sheldon, *Chem. Ind. (London)*, (1990) 212–219.
- [16] A.M. Krstulovic (Ed.), *Chiral Separations by HPLC*, Ellis Horwood, Chichester, 1989.
- [17] A.L. Margolin, *Enzyme Microb. Technol.*, 15 (1993) 266–280.
- [18] C.H. Wong, *Chemtracts Org. Chem.*, 3 (1990) 91–111.
- [19] G.M. Whitesides and C.H. Wong, *Angew. Chem., Int. Ed. Engl.*, 24 (1985) 617–638.
- [20] J.B. Jones, *Tetrahedron*, 42 (1986) 539–553.
- [21] G. Kirchner, M.P. Scollar and A.M. Klibanov, *J. Am. Chem. Soc.*, 107 (1985) 7072–7076.
- [22] Y.F. Wang, J.J. Lalonde, M. Momogan, D.E. Bergbreiter and C.H. Wong, *J. Am. Chem. Soc.*, 110 (1988) 7200–7205.
- [23] B. Cambou and A.M. Klibanov, *Biotechnol Bioeng.*, 26 (1984) 1449–1454.
- [24] G. Langrand, M. Secchi, G. Buono, J. Baratti and C. Triantaphylides, *Tetrahedron Lett.*, 26 (1985) 1857–1860.
- [25] D. Bianchi, P. Cesti and E. Battistel, *J. Org. Chem.*, 53 (1988) 5531–5534.
- [26] K. Laumen, D. Breitgoff and M.P. Schneider, *J. Chem. Soc., Chem. Commun.*, (1988) 1459–1461.
- [27] R.N. Young, Y. Guindon, T.R. Jonnes, A.W. Ford-Hutchinson, P. Belanger, E. Champion, L. Charette, R.N. DeHaven, D. Denis, R. Fortin, R. Frenette, J.Y. Gauthier, J.W. Gillard, M. Kakushima, L.G. Letts, P. Masson, A. Maycock, C. McFarlane, H. Piechuta, S.S. Pong, A. Rosenthal, H. Williams, R. Zamboni, C. Yoakim and J. Rokach, *J. Adv. Prostaglandin Thromboxane Leukotriene Res.*, 16 (1986) 37.
- [28] D.L. Hughes, J.J. Bergan, J.S. Amato, P.J. Reider and E.J.J. Grabowski, *J. Org. Chem.*, 54 (1989) 1787–1788.
- [29] D.L. Hughes, J.J. Bergan, J.S. Amato, M. Bhupathy, J.L. Leazer, J.M. McNamara, D.R. Sidler, P.J. Reider and E.J.J. Grabowski, *J. Org. Chem.* 55 (1990) 6252–6259.
- [30] G.B. Smith, M. Bhupathy, G.C. Dezeny, A.W. Douglas and R.J. Lander, *J. Org. Chem.*, 57 (1992) 4544–4546.
- [31] L. Katz, C. Marcin, L. Zitano, J. King, K. Price, N. Grinberg, M. Bhupathy, J. McNamara, J. Bergan, R. Greasham and M. Chartrain, *J. Ind. Microbiol.*, 11 (1993) 89–94.
- [32] M. Dixon and C.E. Webb, *Enzymes*, Academic Press, New York, 2 edn., 1964, pp. 420–443.
- [33] H.J. Eperson, *Chemical Kinetics and Reaction Mechanisms*, McGraw-Hill, New York, 1981, pp. 12–16.
- [34] J.M. Clark Jr., and R.L. Switzer, *Experimental Biochemistry*, Freeman, San Francisco, 1964, 2nd edn., pp. 83–84.
- [35] C. Moeder, N. Grinberg, H.J. Perpall, G. Bicker and P. Tway, *Analyst*, 117 (1992) 767–771.
- [36] J. Ruzicka and E.H. Hansen, *Flow Injection Analysis*, Wiley, New York, 2nd edn., 1988, pp. 37–38.